The Third-Generation Los Alamos Designed 1.5U CubeSat Attitude Determination and Control System: Design and Initial On-Orbit Results

James A. Wren, Michael C. Proicou, Nicholas A. Dallmann, Emily M. Baldwin, Jerry G. Delapp,
Michael Gacusan, Kimberly K. Katko, John P. Martniez, Hannah D. Mohr, Donathan J. Ortega,
Michael W. Rabin, Edward B. Schaller, Daniel N. Seitz, Terra G. D. Shepherd, Paul S. Stein,
Erica A. Sullivan, Justin L. Tripp, Adam Warniment, Robert M. Wheat
Los Alamos National Laboratory
P.O. Box 1663, Los Alamos, NM 87545; 505-665-5941
jwren@lanl.gov

ABSTRACT

The 3rd Generation 1.5U CubeSat designed at Los Alamos National Laboratory (LANL) contains a compact 3-axis attitude determination and control system (ADCS) to support the pointing requirements of a deployable high-gain antenna. The hardware and software for the ADCS system were designed and built entirely at LANL with the goal of minimizing the size requirements and unit costs. The satellites employ a combination of magnetometers, sun-vector sensors, solid-state gyroscopes, and a star-field sensor for attitude determination. Attitude actuation is accomplished using either 3 magnetic torque rods or 4 momentum wheels arranged in a pyramid configuration. The on-board ADCS processor runs a real-time operating system that is fully reprogrammable while in orbit. The first two units were launched in November 2016 and both units are currently operating in orbit. We will present the design of the hardware and software systems, pre-launch testing and simulation, and initial on-orbit results.

INTRODUCTION

The Los Alamos National Laboratory (LANL) began constructing CubeSats[12] in 2008 with the intent to develop a platform that would enable innovation in the laboratory's science and national security missions[1].

In December, 2010, the first four LANL Designed CubeSats were launched into a 300 km orbit at an inclination of 34.5° on a SpaceX Falcon 9. The development of these satellites took about 6 months. The primary goal of this initial program was to demonstrate the ability to build and launch a satellite quickly and at a very low cost. The satellites were designed to be used by non-experts to demonstrate communication capability with an extremely modest ground station footprint. All four satellites and ground stations performed flawlessly throughout their three-week design lifetime.

In November, 2013 eight LANL 2nd Generation (Block 1) CubeSats were launched into a circular 500 km orbit at an inclination of 40.5° on a Minotaur 1 rocket. These units had several improvements over the previous generation including:

1. Fully encrypted communications using new a high-gain and high-bandwith antenna.

2. An attitude control system for both sun pointing and target tracking.

3. Configured and scripted tasking of the satellite.

4. Remote, networked control of ground stations.

5. Code upload and reprogramming of all microprocessors and software defined radio (SDR) FPGAs while in orbit.

The Block 1 satellites successfully demonstrated active attitude control and communications with a high-gain deployable helical antenna in a 1.5U CubeSat format. The satellites met all of their design goals, but many lessons were learned in the process. All satellites re-entered the atmosphere in early 2016.

The 3rd Generation (Block 2) LANL CubeSats (Figure 1) were designed to address many of the lessons that were learned in Block 1. Two Block 2 satellites were launched in November 2016 and are now operating in orbit. These satellites are very similar to the Block 1 design but with several upgrades to the system. In addition to changes to the radio systems to improve communication data rates, there were several improvements to the attitude determination and control system (ADCS). These improvements include:

1. Larger diameter momentum wheels for improved momentum storage.

2. Magnetic torque rods to enable low-power sun pointing and dissipate angular momentum

imparted during deployment or by differential drag on the satellite.

3. A star-field sensor (SFS) capable of providing attitude solutions to 0.01° accuracy.
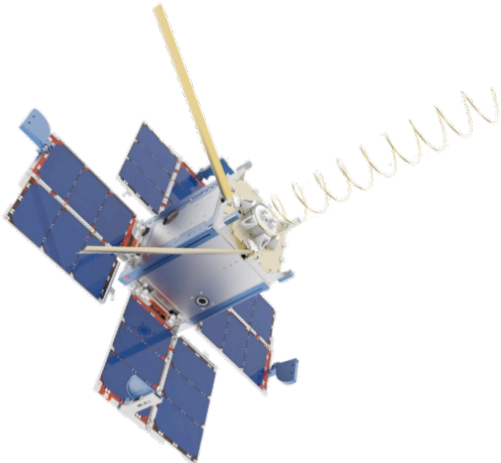

Figure 1: Los Alamos Designed 3rd Generation CubeSat (Block 2)

Another improvement in the Block 2 design is the capability to host payloads. Given the 1.5U form factor of the Block 2 bus, an additional 1.5U payload would still allow the satellite to fit within a standard 3U dispenser. The solar panels were designed to provide 24 W of power when normal to the sun, leaving ample margin to power a payload even during a ground station pass, during which the primary bus consumes 13 W of power. The batteries have 109 kJ of capacity to power the system when the satellite is in darkness. Finally, the momentum wheels, each with a moment of inertia of 1.68×10^{-5} kgm^2, are sized to allow ground target pointing while hosting a 1.5U payload.

A 51-pin connector and a custom interposer printed circuit board provide access to the satellite's subsystems and internal power rails. A second connector provides access to the battery and charging circuitry. The payload would be attached to the spacecraft at the end located at the opposite side from the radio antennas. An additional benefit of the payload connectors is that they also provide an easy, non-invasive, communication route to the satellite's subsystems after the satellite is fully assembled.

The pointing requirement of the satellite is primarily driven by the directional high-gain helical antenna (Figure 2). The high-gain radio operates at about 2 GHz with a right-hand circular polarization. The antenna gain falls off 1 dB at about a 10° beam width

and 3 dB at about a 35° beam width. The current performance goal of the ADCS system is to point with an accuracy of at least 15° to ensure reliable operation of the high-gain communication system.
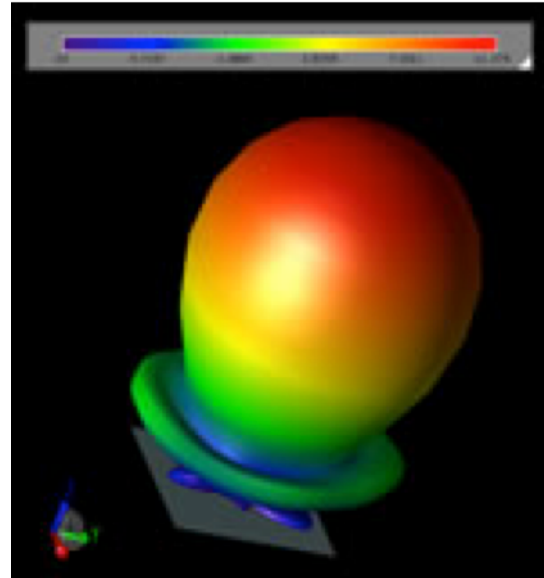

Figure 2: High-Gain Antenna Beam Pattern

ADCS HARDWARE DESIGN

The Los Alamos CubeSat architecture has been developed to maximize accessibility and modularity. The system breaks into three major pieces (Figure 3). The 'top' is the housing for the analog processing and antennas. The 'middle' is the card cage housing the software defined radios (SDRs), command and data handling (CDH), and attitude determination and control system (ADCS) subsystems. The 'bottom' is the power system. All subsystems in all three pieces are connected to each other by a single backplane. It is intended that each subsystem be as independently testable as possible.

Within the Block 2 CubeSat are 5 independent processing cards to drive the CDH, ADCS, Low-Band SDR, High-Band SDR, and the SFS. Each card is controlled by a 32-bit ARM Cortex-M4 processor with 1 MB of flash memory. Currently the processor is clocked at 168 MHz. The processor is attached to an external SRAM chip providing an additional 8 MB of memory and an external flash chip providing 1 GB of storage. The processor is also paired with a Field-Programmable Gate Array (FPGA) from Microsemi that controls many of the autonomous functions of the satellite. The FPGA provides a memory-mapped interface to many of the external devices as well as

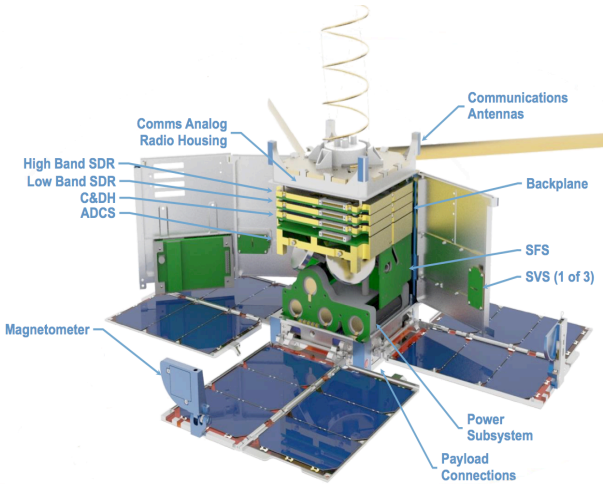watchdog timers that will reboot the processor in the event of a system fault.

Figure 3: Exploded View of the Block 2 CubeSat

Due to the 1.5U form factor of the Los Alamos CubeSat, the ADCS subsystem was designed to be very compact (Figure 4). The primary ADCS subsystem contains the processing circuit board along with four momentum wheels and three torque rods for attitude actuation. The ADCS circuit board layout incorporates holes in the circuit board to allow the momentum wheels to pass through the plane of the board. The primary ADCS unit also contains a solid-state gyroscope mounted on the momentum wheel carriage. The thickness of the primary ADCS unit is about 4 cm (1/3 of a CubeSat standard unit). Three small sun-vector sensors (SVS) are attached to the satellite body and two magnetometers are located at the ends of two of the solar panels. Finally, a star-field sensor (SFS) is located just below the primary ADCS unit. A circular cutout in the backplane circuit board allows the SFS an unobstructed view out of the satellite.
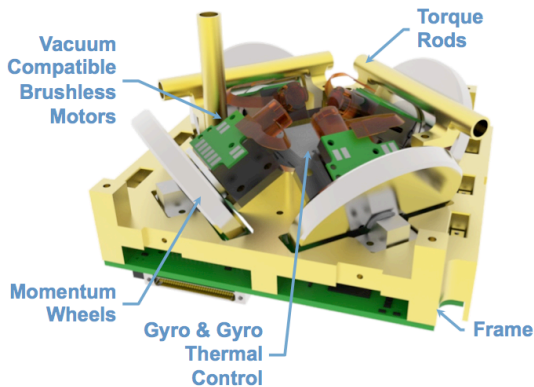

Figure 4: ADCS Subsystem

The body coordinates of the spacecraft are chosen so that the high-gain helical antenna is considered the +z axis. The SVS units are located on the +x, -x, and –z axes. The magnetometers are located on the +y and –y solar panels. The SFS points along the –y axis of the spacecraft.

ADCS SOFTWARE DESIGN

The processors run a real-time operating system (RTOS) provided by ARM's Keil MDK development package (Figure 5). The internal flash memory of the ARM processor is divided into three banks. Bank 0 is 208 MB in size and holds the recovery code that is loaded prior to launch. The Bank 0 code is not intended to be modified after launch and represents the safe recovery mode after a system reset. The other two banks, A and B, are each 384 MB in size and contain the operational flight code that can be updated while on-orbit. Code updates are loaded onto Banks A and B in an alternating manner. The system of alternating updates allows easy fallback to the previous version if there is a problem with the most recent code update.

The flight control code is written in the C programming language. Each of the satellite subsystems share a common set of code libraries for performing operating system functions, filesystem operations, inter-board communications, and common user interface functions. Additionally we have developed a software library, NavLib, which contains functions for performing common mathematical operations such as linear algebra, orbit determination, astronomical ephemeris, and statistical modeling. The code base is maintained within a Mercurial revision control system.
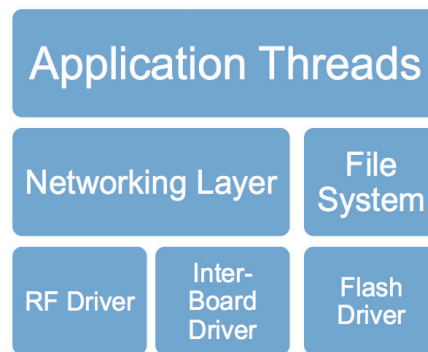

Figure 5: Multi-Threaded

RTOS Architecture

The ADCS system is driven by a multi-threaded control loop running on its ARM processor. One thread is dedicated to listening for incoming commands from the CDH or from the ground station via the radios. Another thread is dedicated to running a 1 Hz control loop that determines the attitude of the satellite and then updates the attitude actuators to execute the required attitude maneuver.

ATTITUDE DETERMINATION

The Block 2 design uses two primary methods for attitude determination. The first is by using the SVS in combination with the magnetometers. The second is through the use of the SFS. The SVS/magnetometer solution, when available, is produced in near real-time. The SFS solution is much more accurate, but will be at least 10 seconds old.

Neither the SVS or magnetometers can provide a complete attitude solution by themselves, and therefore only work in combination with each other. The sun-vector is determined by one of three pinhole cameras located in the +x, -x, and –z body axes respectively. The sun position is then converted to inertial coordinates through the use of a sun ephemeris formula and the current time. The magnetometer data provides the second reference point for the attitude solution. The Earth's magnetic field intensity and direction are measured independently by four magnetometers onboard the spacecraft. Two magnetometers are located on the +y and –y solar panels and the third and fourth are located within the body of the spacecraft. The magnetic field is measured in body coordinates and then converted to inertial coordinates by comparison to the WMM[2] magnetic field model. This comparison requires knowledge of the current time and also the current satellite geo-location. The TRIAD[3] algorithm is used to combine the sun-vector and magnetometer measurements into the full satellite attitude solution in inertial coordinates.

Because the SVS/magnetometer attitude solution depends on knowledge of the time and spacecraft position, the spacecraft must have the clock set and a current orbital element set uploaded. Currently the spacecraft clock is not set until the first successful ground contact. Shortly thereafter, the current TLE is uploaded to the spacecraft. Only then will the onboard algorithm be able to determine the attitude using the SVS/magnetometer method. Another disadvantage of the SVS/magnetometer method is that it only works during periods when the spacecraft is in sunlight.

Unlike the SVS and magnetometer sensors, the SFS provides the ability to determine the attitude without knowledge of the current time or geo-location of the spacecraft. The SFS operates by taking an image of the star-field and comparing to an on-board star catalog. If a valid catalog match is found, the attitude is determined by applying the QUEST[4] algorithm to all of the positively matched stars in the field. Typical SFS attitude solutions are accurate to 0.01 degrees.

The SFS has several drawbacks. The SFS currently requires the satellite to be rotating at less than a few degrees per second in order to limit smearing of the star-field. The SFS image must also not contain the Sun, Moon, or Earth within its field of view. Finally, if an attitude solution is found it will generally be 10-200 seconds old. If an attitude estimate is currently available, then the time required for subsequent SFS solutions is about 10 seconds.

Finally, the solid-state gyroscopes are used to propagate the attitude solution when it is not currently available by other means. The magnetometer data is essentially always available, but the SVS data must be propagated when the sun is not in the field of view of any of the three SVS sensors, either because the current attitude of the spacecraft puts the sun out of the field of view or because the spacecraft is in the dark phase of its orbit. The attitude solution from the SFS must always be propagated using the gyroscopes because it is at least 10 seconds old, and often much older. The point at which the propagated SFS solution is no longer better than a current SVS/magnetometer solution depends on the drift rate of the gyroscopes.

ATTITUDE ACTUATION

There are two methods by which the attitude of the spacecraft is controlled: momentum wheels and magnetic torque rods. The momentum wheels provide the necessary torque to perform ground target tracking but they consume much more power and have limited lifetimes. The magnetic torque rods consume less power, but provide much less torque. As a result, the torque rods can only be used for de-tumbling, static sun pointing, or nadir pointing operations.

The momentum wheel system is composed of four wheels arranged in a pyramid configuration. The motor for each wheel is capable of producing about 1 mNm of torque. The individual motor speeds are controlled by the FPGA which runs a proportional-derivative (PD) control loop. The desired motor torques are chosen by determining the error angle between the command attitude and the current attitude solution. A PD control loop is applied to the attitude error angle to generate the desired torque setting. The individual wheels are then driven to the required speed setting to generate the requested overall torque on the spacecraft.

The magnetic torque rods operate using the same control law as the motors to determine the desired torque on the spacecraft. The magnetic field is measured using the magnetometers and the appropriate current is applied to the torque rods to generate the requested torque on the spacecraft. However, the maximum torque generated by each individual rod is only about 10 µNm, two orders of magnitude less than the momentum wheels. In practical use, the current draw of each individual rod is limited to 0.1 A which limits the torque any individual rod may apply to about 2 µNm.

SUN VECTOR SENSORS

The SVS units used on Block 2 are the same that were used successfully in the previous Block 1 generation. The sensor is a Duo-Lateral Position Sensitive Photodiode (PSD) from First Sensor, Inc. The PSD measures 10 x 10 mm and is located 2.57 mm below the pinhole, giving a field of view of about 120 degrees. The sun-vector is derived from the relationship between two anodes (the x-axis) and two cathodes (the y-axis). The current from the PSD anodes and cathodes is converted to a voltage and read through the Microsemi FPGA.
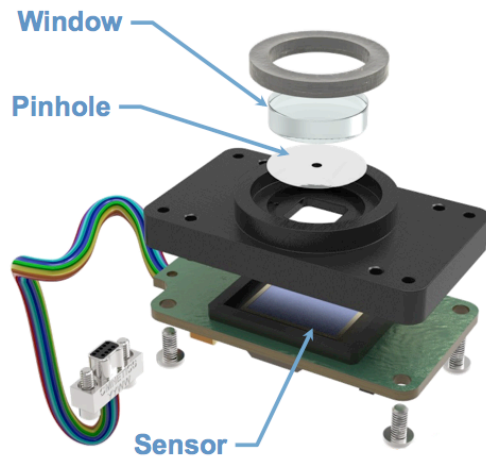

Figure 6: Sun-Vector Sensor

Three SVS units are placed on the spacecraft body in the +x, -x, and –z directions respectively. Combined the SVS sensors cover nearly ¾ of the full sky.

A calibration testing fixture was developed to improve the accuracy of the SVS results. The light source for the test fixture is a 3 mW laser mounted on an optical bench within a light tight housing. The SVS is placed

on a 2-axis motorized mount allowing the SVS to be rotated perpendicular to oncoming laser beam. Position dependent calibration offsets can then be derived by comparing the motorized mount settings to the "sun" angle computed by the SVS (Figure 7).
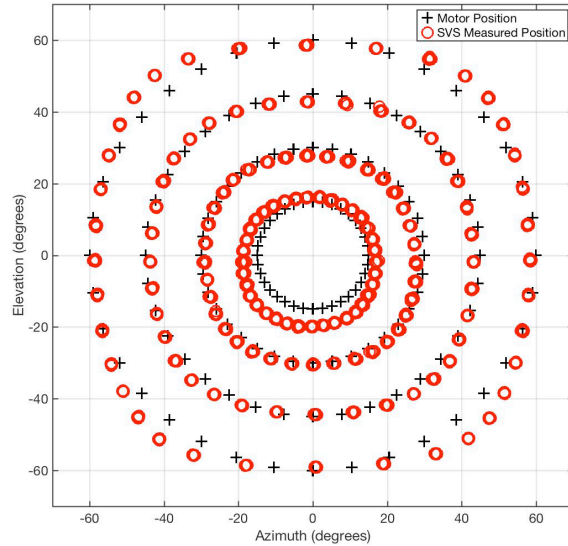

Figure 7: Example Results from a SVS Calibration Run

MAGNETOMETERS

The Block 2 design has 4 magnetometers. Two are located at the ends the +y and –y solar panels. Two more are located within the body of the spacecraft. The magnetometers are designed to measure both the magnitude of the Earth's magnetic field and direction with 1º to 2º accuracy.

The magnetometers report their measurements via an I^{2}C interface. The measurements are 12-bit values with a resolution of 2 milli-Gauss and a range of ±8 Gauss. The magnetometers have a maximum 160 Hz output rate and are read by the FPGA which then provides the data via a memory-mapped interface to the ARM processor.

Attitude determination with the magnetometers is performed by comparing the readings to the World Magnetic Model (WMM)[2] produced by the National Geospatial-Intelligence Agency (NGA) and the United Kingdom's Defense Geographic Centre (DGC). The model is updated every 5 years. Currently the 2015 WMM model is computed by our NavLib Library for use by the ADCS control software.

STAR-FIELD SENSOR

The SFS module (Figure 8) is based on a Python 1300 image sensor from ON Semiconductor, Inc. The sensor is a high-sensitivity monochrome CMOS chip with a 1280x1024 pixel array (1.3 Mpix). The Python sensor is paired with a 16 mm f2.0 s-mount lens from Marshall Electronics, Inc. The resulting field of view is 21.7 x 17.5 degrees.

The SFS is controlled by the same ARM processor used for the CDH, ADCS, and SDR boards. The Python sensor is connected to the Digital Camera Interface (DCMI) on the ARM processor which reads the image to the external SRAM. Image readout takes about 2.4 seconds; slower than expected due to reported memory errors when transferring the image at higher speeds to the external SRAM.

After the image is read out, it is scanned for stars. The noise floor of the image is determined by taking the median of a representative portion of the image. A threshold is then set at about 3σ above the noise level. Connected groups of pixels above the threshold level are merged into sources. The centroid of each source is computed using a simple weighted mean. The resulting object list contains the image coordinates, total source counts, and number of pixels above threshold for each source. The source extraction algorithm currently takes about 6.7 seconds for the full 1.3 Mpix image.
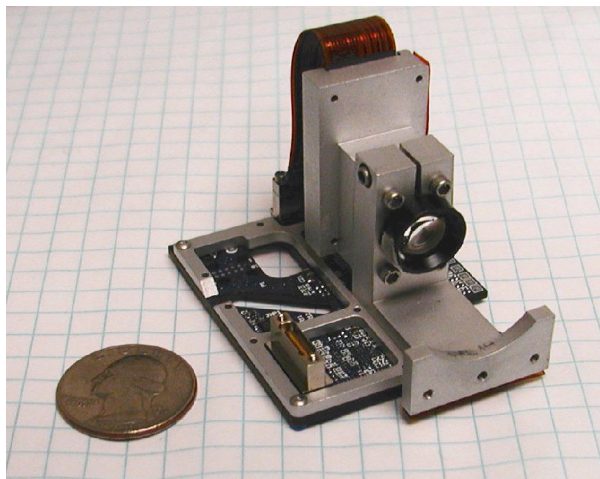

Figure 8: Star-Field Sensor

The object list is then compared to a star catalog that was loaded onto the ARM filesystem prior to launch. The reference star catalog is based on the Tycho-2[5] catalog with a cutoff on the faint end at an astronomical visual magnitude of 10. A "search catalog" derived from the Tycho-2 catalog is also stored on the file system. The search catalog contains star pairs with separations less than 17 degrees and magnitudes less than 5.0. The image is calibrated by taking pairs of stars from the object list and comparing to star pairs from the search catalog with a similar separation. For each image and catalog pair combination, a test rotation matrix is computed using the TRIAD algorithm. The test rotation is applied to the other stars in the object list and if more than 5 stars are within 0.001 radians of a catalog star then the rotation is considered a successful match. The QUEST algorithm is then used to compute the final rotation from body to inertial coordinates using all of the stars within the image that matched a catalog star.

Image calibration takes from 0.5 to 200 seconds depending on how many catalog pairs were required to be tested before a successful match. After a successful match, the attitude determination algorithm attempts to match the next image to the same catalog reference stars. If the spacecraft hasn't rotated them out of the field of view since the last solution, then the new image should be calibrated in less than a second.

A set of 277 test images were taken with a test SFS module from the Fenton Hill observatory site near Los Alamos, NM. The exposure times ranged from 200 ms to 1000 ms. A Matlab version of the software was used to test the extraction and calibration algorithm. The software was able to successfully calibrate all the test images. The resulting accuracy of the attitude solution averaged 0.011 ± 0.002 degrees when compared to the Tycho-2 star catalog.

GYROSCOPES

During periods when a current attitude solution is not available, the attitude must be propagated using the gyroscopes. The current attitude solution will not be available during gaps in the Sun coverage by the SVS sensors and while the SFS is searching for a star-field match. Gaps in the SVS coverage can last up to 32 minutes, when the spacecraft is passing over the nighttime side of the Earth. Gaps in the SFS coverage can potentially be indefinite if the spacecraft is rotating too quickly for a solution to be determined. The minimum current gap in the SFS coverage is 10 seconds. Therefore accurate gyroscope propagation is essential.

Two gyroscopes are mounted inside the spacecraft. The first is located on the center of the motor mounting block (Figure 9), while the second is located on the ADCS circuit board. The sensor used is the L3G4200D from ST Micro and it provides angular rates about all 3 axes. The resolution of the gyroscopes is 8.75 milli-degrees/s with a range up to 250 degrees/s.
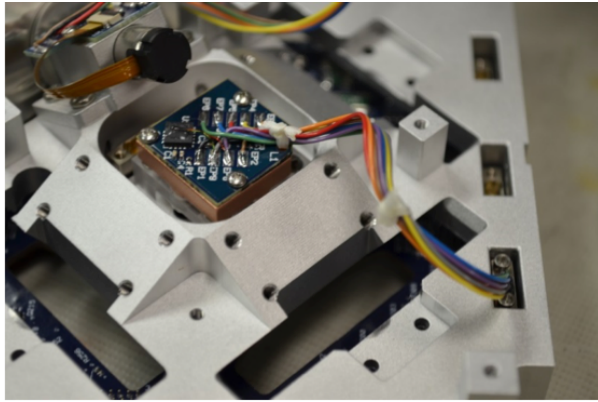
Figure 9: Gyro PCB and Thermal Isolation Block Mounted on the Momentum Wheel Fixture

The gyroscope datasheet claims to have an Allan Variance[6] of 1.38 degrees/√hour. We tested a gyroscope over a 3 day time period at 100 Hz and were able to confirm the datasheet value (Figure 10). Our tests showed a variance of about 0.014 degrees/√Hz per axis. This should translate to 0.024 degrees/√Hz if all three axes are added in quadrature. Multiplying by 60 gives a value of 1.45 degrees/√hour.
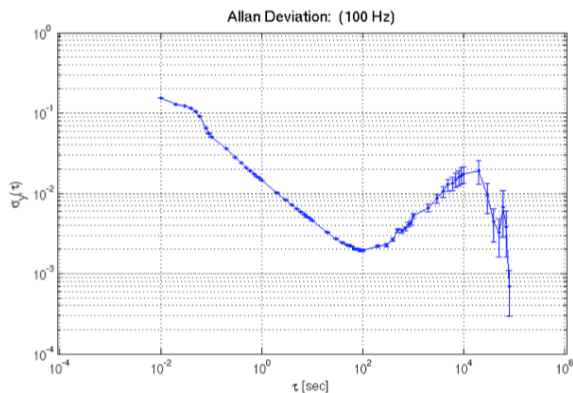

Figure 10: Allan Variance Along the Z-Axis

During testing of the Block 1 generation of satellites, we discovered a larger than expected temperature dependence of the gyroscope zero-point level. The Block 2 design is now configured to use a temperature dependent fit of the gyroscope zero point settings, allowing much improved accuracy (Figure 11).
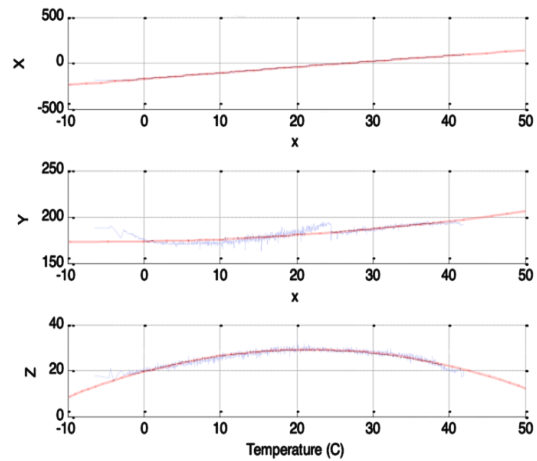

Figure 11: Gyroscope Temperature Compensation Fit

MOMENTUM WHEELS

The momentum wheel system (Figure 12) is based around a Maxon 384406 Ø8 mm motor. The motor is a brushless DC system with Hall sensors. The motors are modified to have space-rated Castrol Braycote Micronic 601 EF as a lubricant.

Each motor is commutated by the FPGA located on the ADCS circuit board. The FPGA also uses pulse-width modulation to regulate the speed according to a simple proportional-derivative (PD) control law. The gain for the control law is configurable on-orbit if necessary. The FPGA also provides a memory-mapped interface for the ARM processor to read and adjust the motor speeds.
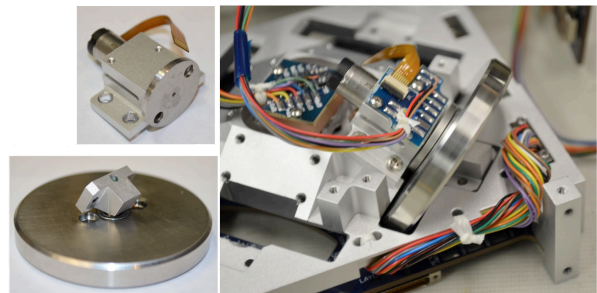

Figure 12: Momentum Wheel Assembly

Each wheel is 1.75 inches in diameter and 0.225 inches thick giving a moment of inertia of 1.68×10^{-5} kgm^2. This is a factor of nearly 40 over the Block 1 generation.

The wheels are arranged in a pyramid formation with a 20° elevation angle. Two motors are run clockwise and two counter-clockwise for a zero net-torque balance when at constant angular velocity.

The control law[7] used to command the motors is:

$$\tau = -\Omega J \omega + D\omega + sKq_e \qquad (1)$$

Where τ is the command torque, J is the moment of inertia of the spacecraft, ω is the angular velocity of the spacecraft, q_e is the quaternion error vector between the command and determined attitude, and s is the sign of the scalar quaternion error term. Ω is the skew-symmetric angular velocity matrix, given by the following formula:

$$\Omega = \begin{bmatrix} 0 & -\omega_3 & \omega_2 \\ \omega_3 & 0 & -\omega_1 \\ -\omega_2 & \omega_1 & 0 \end{bmatrix} \qquad (2)$$

The terms K and D in equation 1 are the proportional and derivative gains of the control system. The system is critically damped when the settling time, T, is equal to $8/\omega_n$ where ω_n is the natural oscillation frequency of the system. For a desired settling time, the gains can be found according to the following formula:

$$K = 2\omega_n^2$$
$$D = \sqrt{2K} \qquad (3)$$

The command torque from equation 1 is then transformed to individual motor velocity commands by a torque distribution matrix.

In order to determine the control gains that work for our momentum wheel control system, we developed a hardware-in-the-loop (HWIL) test. This test is based on a Matlab program that simulates a torque command sequence for a given orbital scenario. Given an initial set of conditions such as orbit position, satellite attitude, rotation rate, and a list of ground targets, the simulation will determine a command attitude quaternion. The error quaternion is derived and the command torque is calculated according to equation 1.

The command motor velocities are then determined using the torque distribution matrix. These motor velocities are then applied to an actual set of motors configured as they would be on the satellite. The response of the motors is then fed back into the simulation. A new attitude quaternion is calculated using a kinematic propagation based on the measured motor velocities from the hardware setup. The

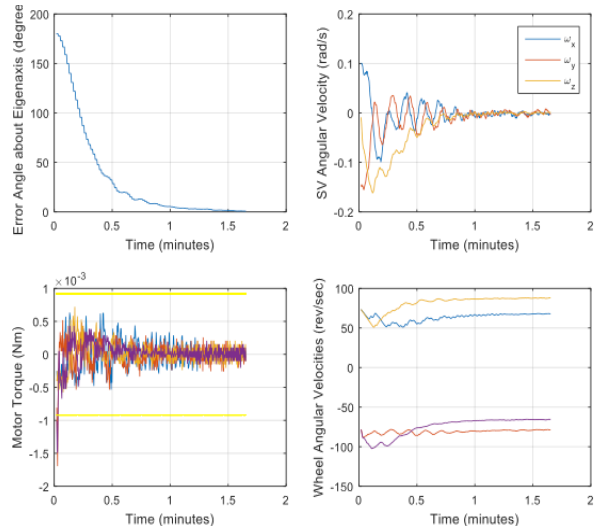command loop is then repeated with the updated "determined" attitude quaternion.

Figure 13: Hardware-In-The-Loop Test Results

Figure 13 shows the results of a HWIL simulation of a 180° rotation using a settling time of 60 seconds. Initial motor velocities were set at 75 rps. The current settling time of the Block 2 satellites in orbit has been lengthened to 120 seconds to relax the torque required of the motors in order to help extend their lifetimes.

MAGNETIC TORQUE RODS

A new feature of the Block 2 satellites is the addition of magnetic torque rods for attitude control (Figure 14). Although much weaker than the momentum wheels, the torque rods have no moving parts and consume much less power than the wheels.

The torque rods for the x and y axes are 5.3 cm long, have a 6.4 mm diameter, and have 815 turns. The core is 1018 steel alloy. The z axis has a shorter torque rod which is 4.4 cm long with 680 turns. The x and y rods produce a dipole moment of $0.596 \times I$ Am^2. The z axis rod produces a dipole moment of $0.412 \times I$ Am^2.

The maximum current draw is about 0.5 A, or 1.8 W at 3.3 V. Assuming a 0.3 Gauss magnetic field, the torque rods generate a maximum torque of about 9 μNm, roughly equivalent to a milligram at the end of a 1 meter lever arm. In practical use, because of the control law dynamics, the torque rods are limited to 0.1 A maximum current draw.

3-axis attitude control using the torque rods is not possible at any given instant in time because the torque rods only act about an axis that is perpendicular to the Earth's magnetic field. However, 3-axis control is

possible over an extended period of time because the orientation of the magnetic field relative the spacecraft's body axes changes as the satellite moves thorough its orbit.

The control law used for commanding the torque rods is the same as for the motors except that we ignore the gyroscopic term on the right side of equation 1.

$$\tau = D\omega + sKq_e \qquad (4)$$

The reason the gyroscopic term can be ignored is that the applied torques are low. Also, the torque rods don't generate enough torque to perform high angular rate maneuvers. As a result, they only need accurate control authority at low rotation rates, for example inertially static Sun pointing.

After the command torque has been derived according to equation 4, a "requested" dipole moment is calculated according to the following formula[8]:

$$m_{req} = \frac{B \times \tau}{|B|^2} \qquad (5)$$

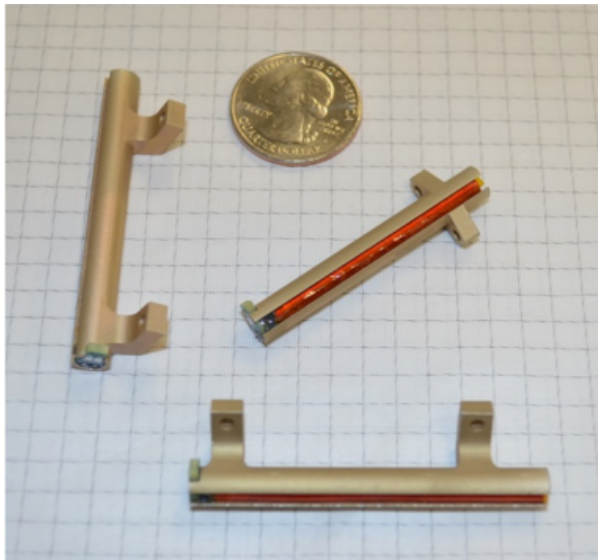The requested dipole moment is then converted to a current command to the appropriate torque rods.

Figure 14: Magnetic Torque Rods

A Matlab simulation of the torque rod behavior was used to determine the appropriate gain settings for the torque rod control law. The IGRF-12[9] model for the Earth's magnetic field was used for the calculations. A settling time of 10 hours was found to work well for our current orbit. Figure 15 shows the results of pointing to an inertially static target (command quaternion

[0,0,0,1]). The initial rotation rate of the spacecraft was set to 1 rpm. The results of the simulation are shown in Figure 14.
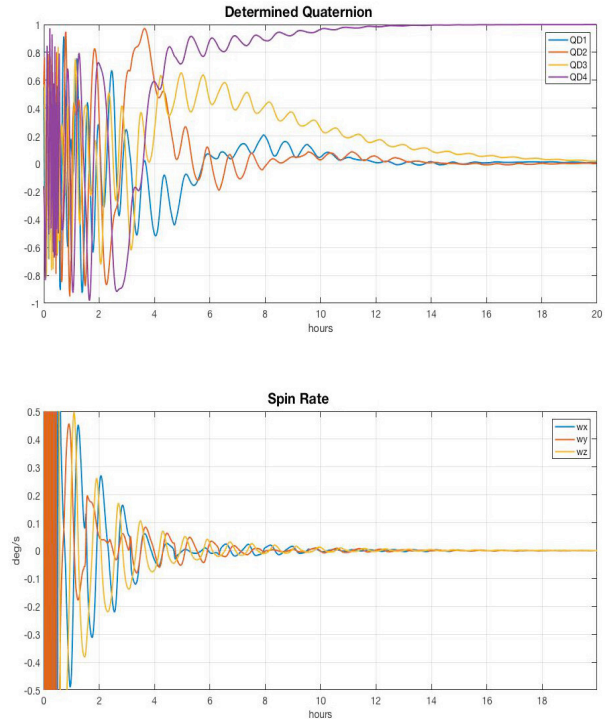

Figure 15: Torque Rod Simulation Results

We have also explored other methods of using the torque rods, such as the B-dot algorithm[10,11] for de-tumbling. However, we prefer to de-tumble by moving directly to sun pointing with the torque rods to avoid settling in an unfavorable attitude for charging the solar panels.

ON-ORBIT RESULTS

Two 3rd Generation (Block 2) Los Alamos Designed CubeSats were launched in November 2016. Both satellites are operating, but we have experienced technical challenges with the power and radio systems that are in the process of being alleviated through on-orbit software updates that are in progress. As a result, the ADCS system has not yet been run in active pointing mode. Active pointing tests are expected to begin in the summer of 2017.
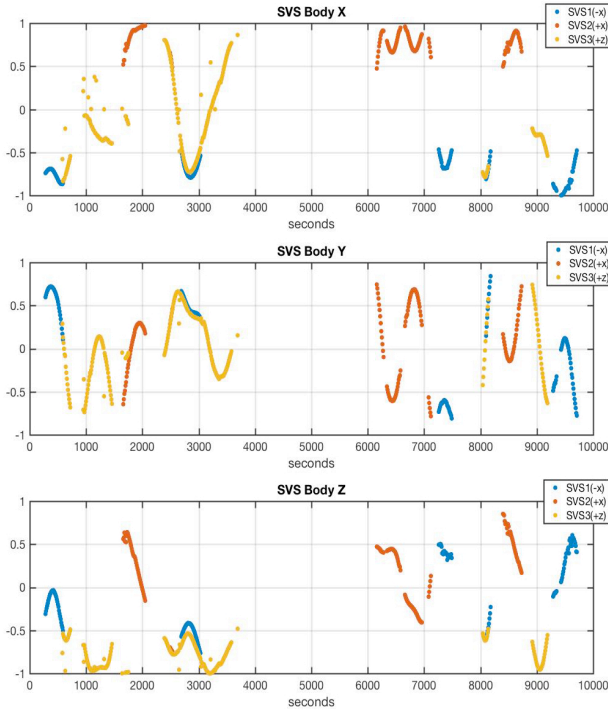
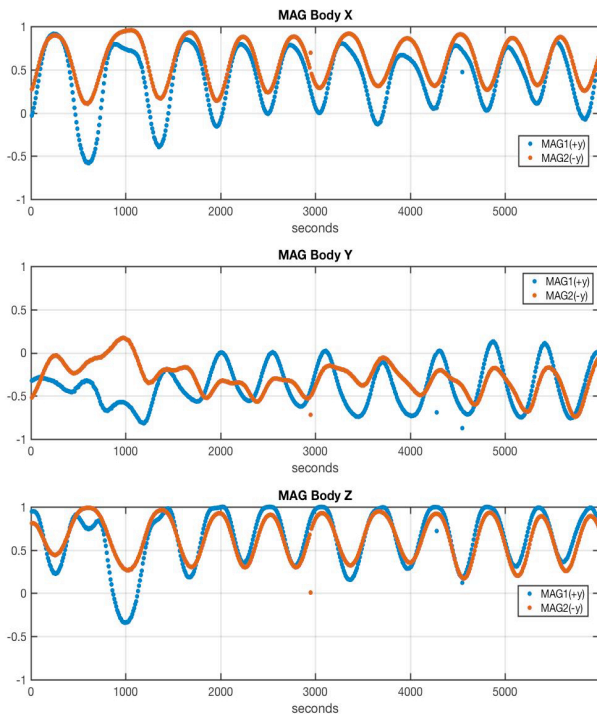**Figure 16: SVS Data from a Block 2 Satellite**

Figure 17: Magnetometer Data from a Block 2 Satellite

ADCS sensor data from the two Block 2 satellites has been successfully downlinked and appears to be working as expected on both satellites. Figure 16 shows the data from one of the satellite's set of SVS sensors on March 24, 2017. Figure 17 shows magnetometer data from the solar panel magnetometers for the other Block 2 satellite taken on May 6, 2017.

Although the momentum wheels are larger in size than the previous Block 1, the motor control algorithm is still largely the same. Figure 18 shows a successful sun-pointing maneuver with the Block 1 satellite. The maneuver works as expected except that motor-2 reaches its saturation point between minutes 1 and 3. The system recovers and completes the maneuver after about 6 minutes. The Block 2 satellites are expected to complete this maneuver in around two minutes because of the larger wheels compared to the Block 1 generation.

The magnetic torque rods have not yet been tested on the Block 2 satellites. As with the momentum wheels, active pointing tests with the torque rods are planned for the summer of 2017.
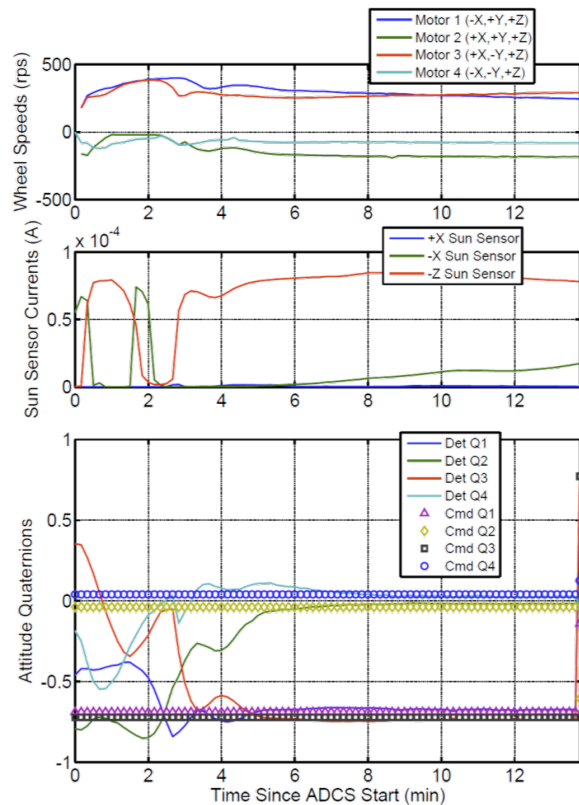

Figure 18: Block 1 On-Orbit Momentum Wheel Maneuver

Conclusion

The 3rd Generation Los Alamos Designed CubeSat (Block 2) builds on the lessons learned from the successful 2nd Generation (Block 1) satellites. The Block 2 design incorporates many improvements to the ADCS subsystem including larger momentum wheels, torque rods, and a star-field sensor.

Two Block 2 satellites were launched in November 2016. The launch and deployment of the satellites was successful and ground communications have been established with both satellites. Technical challenges with the radio communication and power systems are currently being addressed with on-orbit software updates. As a result, testing of the ADCS system has been limited to date. The ADCS has been powered on and the operation of the SVS, magnetometers, and gyroscope sensors has been verified and the sensors are performing as expected on both satellites. Attitude actuation tests are planned for the summer of 2017.

Two additional Block 2 satellites are being delivered for launch later in 2017. These satellites will incorporate several software updates based on lessons learned from ground testing and on-orbit operations with the first two Block 2 satellites.

References

1. Dallmann, N., et al., "An Agile Space Paradigm and the Prometheus CubeSat System," Proceedings of the 29th Annual AIAA/USU Conference on Small Satellites, 2015.

2. Defense Mapping Agency, "Military Specification for the World Magnetic Model (WMM)," Document MIL-W-89500, 1993.

3. Bar-Itzhack, I.Y., R.R. Harman, "Optimized TRIAD algorithm for attitude determination," Journal of guidance, control, and dynamics, vol. 20, No. 1, 1997.

4. Shuster, M. D., Oh, S. D., "Three-Axis Atttitude Determination from Vector Observations," Journal of Guidance, Control, and Dynamics, vol. 4, No. 1, 1981.

5. Hoffleit, D., C. Jaschek, "The bright star catalogue," The Bright Star Catalogue, New Haven: Yale University Observatory (4th Edition), 1982.

6. Allan, D., "Statistics of Atomic Frequency Standards," Proceedings of IEEE, Vol. 54, No. 2, 1966.

7. Wie, B., Weiss, H., and Araposthathis, A., "Quaternion Feedback Regulator for Spacecraft Eigenaxis Rotations," Journal of Guidance, Control, and Dynamics, vol. 12, no. 3, 1989.

8. Graversen, T., et al., "Attitude Control System for AAU CubeSat." Thesis prepared for Aalborg University, Denmark, 2002

9. Thebault, E., et al., "International Geomagnetic Reference Field: the 12th Generation," Earth, Planets, and Space 2015, 67:79.

10. Stickler, A., Alfriend, K., "Elementary Magnetic Attitude Control System," Journal of Spacecraft and Rockets, Vol. 13, 1976

11. Lovera, M., Astolfi, A., "Global Magnetic Attitude Control of Inertially Pointing Spacecraft." Journal of Guidance, Control and Dynamics, Vol. 28, 2005.

12. Heidt, H., et al., "CubeSat: A New Generation of Picosatellite for Eductation and Industry Low-Cost Sapce Experimentation." 14th Annual USU Conference on Small Satellites, 2000.